DOI: 10.18721/JPM.12311
УДК 539.126.3

FEATURES OF SHORT-LIVING NEUTRAL KAON PRODUCTION IN COPPER – GOLD NUCLEI COLLISIONS AT 200 GEV

A.Ya. Berdnikov, Ya.A. Berdnikov, S.V. Zharko, D.O. Kotov, P.V. Radzevich

Peter the Great St. Petersburg Polytechnic University, St. Petersburg, Russian Federation

In this study, invariant transverse momentum spectra and nuclear modification factors of KS mesons produced in collisions of copper and gold nuclei (Cu + Au) at energy of 200 GeV have been measured. The research was carried out using the PHENIX spectrometer located at RHIC. The obtained KS meson nuclear modification factor values were compared with similar ones of η and π^0 mesons along with hadronic jets measured under the same conditions. Moreover, the obtained values mentioned were compared with the corresponding data on KS mesons produced in binary collisions of gold and copper nuclei (Au + Au, Cu + Cu) at energy of 200 GeV as well. An analysis of the derived results pointed to the independence of the jet-quenching effect in the Cu + Au, Cu + Cu and Au + Au collisions at energy of 200 GeV from nuclear overlap form produced in these systems.

Keywords: quark-gluon plasma, jet-quenching, nuclear modification factor, ultrarelativistic heavy nuclei collisions

Citation: Berdnikov A.Ya., Berdnikov Ya.A., Zharko S.V., Kotov D.O., Radzevich P.V., Features of short-living neutral kaon production in copper-gold nuclei collisions at 200 GeV, St. Petersburg Polytechnical State University Journal. Physics and mathematics. 12 (3) (2019) 120–130 DOI: 10.18721/JPM.12311

ОСОБЕННОСТИ РОЖДЕНИЯ КОРОТКОЖИВУЩИХ НЕЙТРАЛЬНЫХ КАОНОВ В СТОЛКНОВЕНИЯХ ЯДЕР МЕДИ И ЗОЛОТА ПРИ ЭНЕРГИИ 200 ГЭВ

А.Я. Бердников, Я.А. Бердников, С.В. Жарко, Д.О. Котов, П.В. Радзевич

Санкт-Петербургский политехнический университет Петра Великого,

Санкт-Петербург, Российская Федерация

В работе проведены измерения инвариантных спектров по поперечному импульсу и факторов ядерной модификации KS-мезонов, рожденных в столкновениях ядер меди и золота (Cu + Au) при энергии 200 ГэВ. Эти исследования выполнены на спектрометре PHENIX, который размещен на коллайдере RHIC. Полученные значения факторов ядерной модификации KS-мезонов сравнивались с соответствующими значениями для π^0- и η-мезонов, а также адронных струй, измеренными при тех же условиях. Кроме того, проведено сравнение полученных факторов с аналогичными данными для KS-мезонов, рожденных в парных столкновениях ядер золота и меди (Au + Au, Cu + Cu) также при энергии 200 ГэВ. Анализ полученных результатов свидетельствует о независимости эффекта гашения адронных струй в указанных системах при энергии 200 ГэВ от реализуемой в них формы области перекрытия ядер.

Ключевые слова: кварк-глюонная плазма, эффект гашения адронных струй, фактор ядерной модификации

Ссылка при цитировании: Бердников А.Я., Бердников Я.А., Жарко С.В., Котов Д.О., Радзевич П.В. Особенности рождения короткоживущих нейтральных каонов в столкновениях ядер меди и золота при энергии 200 ГэВ // Научно-технические ведомости СПбГПУ. Физико-математические науки. 2019. Т. 12. № 3. С. 131–142. DOI: 10.18721/JPM.12311

Introduction

Quantum chromodynamics is a theory describing strong interaction between color-charged quarks and gluons [1]. Color-charged gluons that are carriers of strong interactions generate confinement [1]: in normal conditions, quarks and gluons can only be detected if they combine to form "colorless" hadrons. However, if the temperature increases above 155 MeV, quarks and gluons are released from hadrons and move quasi-freely. Such a system is called quark-gluon plasma (QGP), and quasi-free motion of quarks and gluons is called deconfinement [2].

Modern cosmological models (see, for example, [3–5]) assume that the Universe was in a QGP state in one of the early stages of its evolution, about 10 microseconds after the Big Bang. QGP is produced in laboratory conditions by colliding heavy ultrarelativistic ions (A + A). The first systematic observations pointing to QGP production in A + A collisions were obtained at the Relativistic Heavy Ion Collider (Brookhaven National Laboratory, USA) in collisions of gold nuclei (Au + Au) at center-of-mass energies $\sqrt{s_{NN}}$ = 130 and 200 GeV [6–9]. Further evidence of QGP production was systematically detected in collisions of lead nuclei (Pb + Pb) with $\sqrt{s_{NN}}$ = 2.76 TeV at the Large Hadron Collider (CERN, Switzerland) [10].

An important class of effects corroborating the production of QGP is jet quenching [2, 8–10], that is, strong (by about 5 times in central collisions of gold nuclei) suppression of hadron yield at high transverse momenta, $p_T >$ 4–6 GeV /c, compared with hadron yield in elementary proton-proton collisions (p + p), normalized to the number of inelastic nucleon-nucleon interactions N_{coll} [11].

Jet quenching is quantitatively described with the nuclear modification factor:

$$R_{AA}\left(p_T\right) = \frac{1}{T_{AA}} \frac{dN_{AA}/dp_T}{d\sigma_{pp}/dp_T}, \qquad (1)$$

where dN_{AA}/dp_T is the hadron yield in (A + A) collisions in the given range of transverse momenta; $d\sigma_{AA}/dp_T$ is the inclusive differential cross-section for hadron production in (p + p) collisions; T_{AA} is the average value of the nuclear overlap function [11].

The nuclear overlap function takes the value equal to the ratio of N_{coll} to the total cross section of inelastic nucleon-nucleon scattering ($\sigma_{NN} \approx$ 42.2 mb with $\sqrt{s_{NN}}$ = 200 GeV [11]).

The hadron yield in (A + A) collisions and the number N_{coll} in Eq. (1) are found in a specific class of collision centrality, which is the measure of overlap of two colliding nuclei. Central collisions with a small impact parameter and, as a result, large overlap correspond to centralities of 0–20%; peripheral collisions (with a small overlap and only a small fraction of the nucleons of the incident nuclei participating in the collision) correspond to centralities of 60–90%.

Production of hadrons in the region $p_T >$ 4–6 GeV/c is mainly due to fragmentation of hard partons (quarks or gluons) generated in deep inelastic scattering of valence quarks of colliding nuclei. Fragmentation is the conversion of a hard parton into a jet (hadron beam), occurring as a result of an increase in the total energy of the parton as it exits the nucleus–nucleus interaction containing color charges [1]. Mechanisms of hard partons production in (p + p) collisions are well understood within perturbative QCD [12, 13]: the momentum transferred to the parton in deep inelastic scattering does not change throughout its lifetime and is equal to the total momentum of hadrons in a jet.

Hard partons produced in (A + A) collisions lose some of their energy as they pass through quark-gluon plasma. Energy losses mainly occur due to bremsstrahlung of gluons and elastic scattering by valence partons of the medium. Thus, the momentum of the final jet decreases compared to the momentum transferred to the hard parton as a result of deep inelastic scattering, and the spectrum of hadron fragmentation shifts to lower transverse momenta, compared to the hadron spectrum in (p + p) interactions. No unified theoretical framework has been developed so far to describe parton energy loss in quark-gluon plasma using ab initio methods. However, a range of phenomenological models (see, for example, [14–22]) relying on the measured nuclear modification factor for selecting internal parameters are used for assessing the transport properties of QGP.

Experimental studies have considered the production of different types of hadrons, with systematic analysis of the transport properties of QGP [14–22] depending on particle characteristics (mass, spin, quark composition, etc.) in the final state. For example, a short-lived neutral kaon (K_S meson) is pseudoscalar, i.e., a particle with zero spin and negative spatial parity, containing a strange quark.

Up to the present time, production of K_S mesons has been detected in symmetric systems of binary collisions of ultrarelativistic gold (Au + Au) [23] and copper (Cu + Cu) nuclei [24]. In 2012, the PHENIX experiment [25] at the RHIC collected data for a collision system of nonequivalent nuclei: copper and gold (Cu + Au), at $\sqrt{s_{NN}}$ = 200 GeV. Such a system is the only asymmetric one in collisions of ultrarelativistic heavy nuclei; it is characterized by a special overlap geometry, which has an additional asymmetry along the axis connecting the centers of the nuclei at the moment of their interaction, in contrast to the Cu + Cu and Au + Au systems. Understanding the specifics of production of different particles, in particular, K_S mesons in the Cu + Au collision system, is an important aspect of systematic study of QGP properties that should allow to impose additional restrictions on the parameters of different phenomenological models describing jet quenching.

This paper reports on measurements of invariant production spectra as function of transverse momenta and nuclear modification factors of K_S mesons in the (Cu + Au) collision system at $\sqrt{s_{NN}}$ = 200 GeV.

Experimental procedure

The main characteristics of the detection subsystems of the PHENIX spectrometer are described in [25]. The z coordinate along the beam axis and the centrality of copper and gold ion collisions (referred to as events from now on) were determined using two beam-beam counters (BBC) [26], each located on the beam axis 144 cm away from the nominal collision point and covering a region of $3.1 < |\eta| < 3.9$ units of pseudorapidity.

All events are grouped into centrality classes with a width of 20% (30% for peripheral collisions). The average geometric parameters of nucleus-nucleus collisions for each centrality class (for example, N_{coll}, T_{AA}, the number N_{part} of nucleons participating in the nucleus-nucleus collision) are found by Monte Carlo simulation based on Glauber's theory [11] modeling the response of the BBC counters.

K_S mesons are detected in the $K_S \to \pi^0 + \pi^0$ channel by analyzing the distributions of pairs of candidates for the role of π^0 mesons (π^0 candidates) over invariant mass m_{inv}, determined by the formula

$$m_{inv} = \sqrt{E^2 - \mathbf{p}^2}, \qquad (2)$$

where E, $\mathbf{p}$ are the total energies and momenta of detected π^0 candidates.

In turn, each π^0 candidate is produced in the $\pi^0 \to \gamma + \gamma$ channel, and gamma quanta are detected in the system of electromagnetic calorimeters of the PHENIX spectrometer [27]. The electromagnetic calorimeter consists of eight sectors, each covering 22.5° in the azimuthal angle and 0.7 units in pseudorapidity. Six sectors of the calorimeter are scintillator sampling calorimeters with a lead absorber (referred to as the PbSc subsystem from now on). The other two sectors are lead-glass Cherenkov calorimeters (referred to as the PbGl subsystem). The

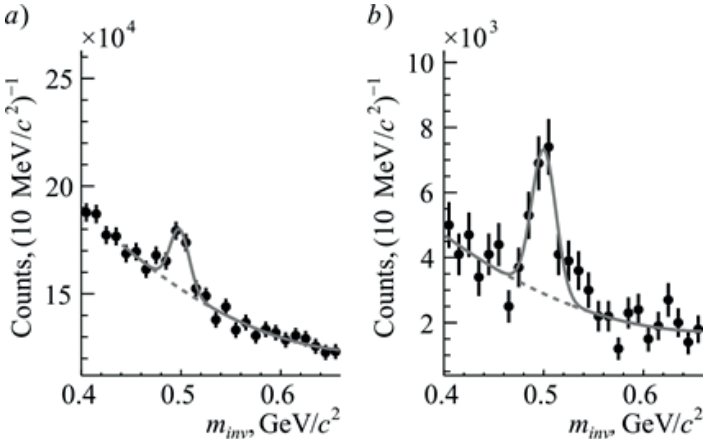

Fig. 1. Example invariant mass distributions of π^0 candidate pairs in 5.0–5.5 (*a*) and 9.0–10.0 (*b*) GeV/*c* ranges.
The peaks correspond to signals from K_S mesons. Circles correspond to experimental data, solid and dashed curves correspond to the "signal + background" and "background" approximation functions, respectively

construction of the electromagnetic calorimeters is described in more detail in [27].

The π^0 candidates are reconstructed by selecting gamma pairs with energies exceeding 0.4 GeV and satisfying the following asymmetry ratio:

$$\frac{\left|E_{\gamma 1} - E_{\gamma 2}\right|}{E_{\gamma 1} + E_{\gamma 2}} < 0.8, \qquad (3)$$

where $E_{\gamma 1}$, $E_{\gamma 2}$ are the gamma energies in a pair.

The lower bound on energy is imposed to reduce the number of false signals in the electromagnetic calorimeter generated by charged hadrons incident on the active area and depositing an average energy of about 300 MeV in the active volume of the calorimeter. Part of hadron showers are also excluded by imposing restrictions on the shape of clusters [27]. Restriction (3) is used to increase the signal ratio from π^0 candidates to background. Additionally, both gammas in a pair should be detected in the same sector of the electromagnetic calorimeter.

The transverse momentum of the π^0 candidate detected in the PbSc (PbGl) subsystem is bounded by 11 (14) GeV/c from above and by 2 GeV/c from below. The lower bound allows to increase the ratio of the signal from K_S mesons to background, and the upper one is introduced to avoid merging of the electromagnetic clusters left by daughter gammas [28].

Next, π^0 candidates are selected within 2σ (σ is the peak width) around the measured masses based on their transverse momentum from π^0 mesons on the invariant mass distribution of gamma pairs; the invariant mass also depends on the transverse momentum of the π^0 candidate. Due to nonlinear effects and limited energy resolution in the electromagnetic calorimeter, the measured masses of π^0 mesons differ from the tabulated values and depend on the transverse momentum. Therefore, after the above-mentioned restrictions are imposed, the energies of the gammas forming the π^0 candidates are adjusted to normalize the measured masses to tabulated values [29]. This procedure makes it possible to increase the signal-to-background ratio of K_S mesons.

Invariant mass distributions of pairs of π^0 candidates are analyzed separately for different transverse momentum ranges and centrality classes. Examples of distributions are shown in Fig. 1, the peaks in the distributions correspond to the signals from K_S mesons. To measure K_S meson yields, the distributions are approximated by a sum consisting of a Gaussian function describing the signal and a second-degree polynomial describing the background (the area around the signal is taken). The number of K_S mesons detected is found as the difference between the sum of samples within the 2σ range around the center of the peak and a polynomial fit integral. The yield, the number of mesons produced at the vertex of nucleus-nucleus collisions, is found by adjusting the number of detected mesons taking into account the finite acceptance and the detector effects in the calorimeter; the kinematic constraints used are also taken into account by estimating the reconstruction efficiency. The reconstruction efficiency is estimated through Monte Carlo simulation of the experimental setup in GEANT3 [30].

The invariant yield of K_S mesons is found by the following formula:

$$I_{KS} = \frac{1}{N_{event}} \frac{d^2N}{2\pi p_T dp_T dy} = \frac{N_{KS}}{2\pi p_T \Delta p_T N_{event} \varepsilon_{rec} \mathrm{BR}}, \qquad (4)$$

where N_{KS} is the number of K_S mesons extracted; ε_{rec} is the reconstruction efficiency; N_{event} the number of events analyzed; BR is the branching ratio for the $K_S \to \pi^0 + \pi^0$ channel, BR = 30.69 ± 0.05 [29].

The systematic uncertainty for measuring the invariant yield of K_S mesons is estimated by comparing the standard yields with the values obtained by varying the approximation parameters of invariant mass distributions, with simulation data (for example, the absolute energy scale and the energy resolution of the calorimeter) and the constraints used. The systematic uncertainty largely originates from the approximation parameters chosen for invariant mass distributions for pairs of π^0 candidates and photon conversion in the detector materials (5.2%). The main approximation parameters are the fitting range, the order of the polynomial for describing the background, the signal integration range. The systematic uncertainty resulting from peak fitting is 10–15%, 8–12%, 18–25% in regions of low, intermediate and high transverse momenta, respectively.

Results and discussion

Fig. 2 shows the invariant spectra for production of K_S mesons depending on their transverse momentum, measured in different centrality classes of Cu + Au collisions at

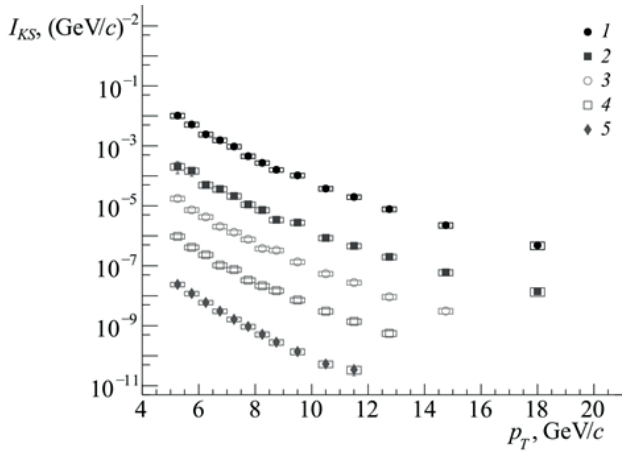

Fig. 2. Invariant spectra for K_S meson production as function of transverse momentum in (Cu + Au) collisions in different centrality classes, %: 0–20 (*2*), 20–40 (*3*), 40–60 (*4*), 60–90 (*5*), and without centrality specified (*1*). The points are scaled for clarity by 10^1 (*2*), 10^0 (*3*), 10^{-1} (*4*), 10^{-2} (*5*), 10^3 (*1*)

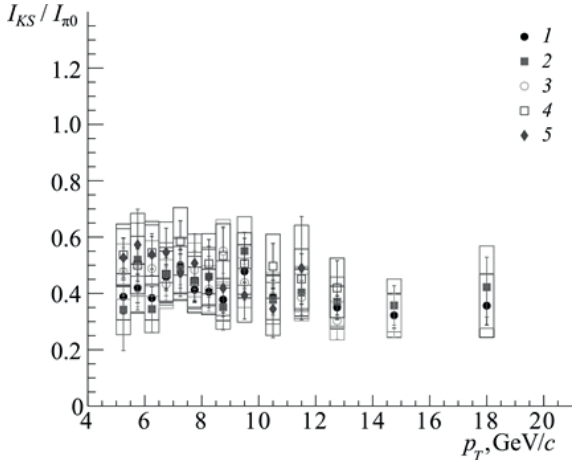

Fig. 3. $I_{KS}/I_{\pi 0}$ ratios as functions of transverse momentum in (Cu + Au) collisions in different centrality classes; the symbols are numbered the same as in Fig. 2

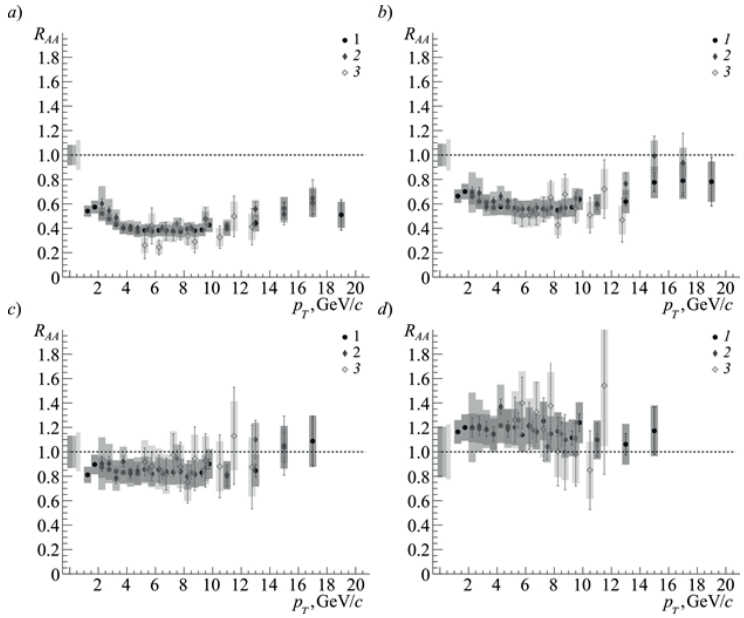

Fig. 4. Nuclear modification factors of π^0 (*1*), η (*2*) [28, 31] and K_S (*3*) mesons as functions of transverse momentum in (Cu + Au) collisions in different centrality classes,%: 0–20 (*a*), 20–40 (*b*), 40–60 (*c*), 60–90 (*d*)

$\sqrt{s_{NN}}$ = 200 GeV. The lower bound in the range of transverse momenta was introduced because it was impossible to separate the signal from the background. The upper bound is introduced because the amount of data is insufficient for measuring the yields. The bars and boxes around the experimental points correspond to the absolute values of statistical and systematic measurement uncertainties.

Fig. 3 shows the ratios of K_S meson to π^0 meson ($I_{KS}/I_{\pi 0}$) yields, measured in different transverse momentum ranges and centrality classes of Cu + Au collisions at energy $\sqrt{s_{NN}}$ = 200 GeV. The π^0 meson yields, previously measured in (Cu + Au) collisions [28, 31], are used as the denominator. Relative statistical and systematic uncertainties for the $I_{KS}/I_{\pi 0}$ ratios are found as the quadratic sum of relative uncertainties in measuring K_S and π^0 meson yields. The measured ratios are independent of the transverse momentum and centrality of the collisions within the measurement uncertainty and are of the order of $I_{KS}/I_{\pi 0} \approx 0.4-0.5$, equal to the ratios measured earlier in the PHENIX experiment in collisions of deuterium and gold nuclei (d + Au) and binary collisions of copper nuclei (Cu + Cu) at $\sqrt{s_{NN}}$ = 200 GeV [24].

Fig. 4 shows a comparison of nuclear modification factors of π^0, η [28, 31] and K_S mesons measured in Cu + Au collisions at $\sqrt{s_{NN}}$ = 200 GeV. The boxes around the points correspond to the absolute values of the systematic mea-

Table

Main interaction parameters in Cu + Au collisions for different centrality classes

Centrality class, %	N_{coll}	N_{part}	T_{AA},(mbn)$^{-1}$
0–20	314	155	7.50
20–40	129	80	3.10
40 – 60	42	35	1.00
60–90	7.6	8.9	0.18
Centrality not specified	107	61	2.50

Notations: N_{coll} is the average number of inelastic nucleon-nucleon interactions; N_{part} is the average number of nucleons participating in a nucleus-nucleus collision; T_{AA} is the average value of the nuclear overlap function.

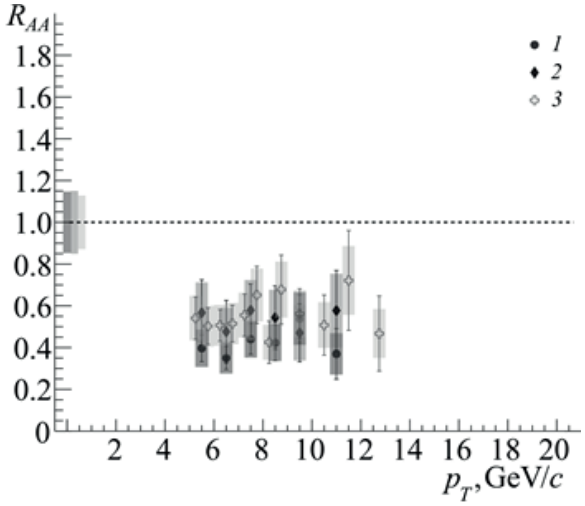

Fig. 5. Nuclear modification factor of K_S mesons (*3*) as function of transverse momentum in Au + Au (N_{part} = 102, centrality class 20–60% [23]) (*1*), Cu + Cu (N_{part} = 85, 0–20% [24]) (*2*) and Cu + Au (N_{part} = 80, 20–40%) (*3*) collisions

surement uncertainty whose correlation in transverse momentum is unknown. The boxes near unity correspond to the relative magnitude of the systematic uncertainty, fully correlated in transverse momentum. The nuclear modification factors of K_S mesons were measured using the differential cross-sections of K_S mesons in ($p + p$) interactions at $\sqrt{s_{NN}} = 200$ GeV given in [32]. The numbers N_{coll} for different centrality classes of Cu + Au collisions are given in Table.

The nuclear modification factors of π^0, η [28, 31] and K_S mesons in (Cu + Au) - collisions coincide within the measurement uncertainty in different transverse momentum ranges and centrality classes. In addition, the nuclear modification factors of π^0, η [28, 31] and K_S mesons in (Cu + Au) collisions ($p_T >$ 10 GeV/c) are equal to those for the jets measured in the corresponding centrality classes of (Cu + Au) collisions [33]. The nuclear modification factor does not depend on the type of mesons in the region $p_T > 4$–6 GeV/c (π^0, η, or K_S), suggesting that jet quenching in (Cu + Au) collisions occurs at the parton level before fragmentation.

The nuclear modification factors of π^0, η, and K_S mesons in central collisions (0–20%) take values of about 0.4 (the value is suppressed by about two times compared with the normalized yield in ($p + p$) interactions at the same energy $\sqrt{s_{NN}} = 200$ GeV) in the region of intermediate transverse momenta (4–10 GeV).

Fig. 5 shows a comparison of nuclear modification factors of K_S mesons measured in Cu + Au, Au + Au [23] and Cu + Cu [24] systems at $\sqrt{s_{NN}} = 200$ GeV, in different transverse ranges, with N_{part} of the order of 100. Notations for the measurement uncertainty are the same as in Fig. 4. Nuclear modification factors of K_S mesons measured in these systems of nucleus-nucleus collisions coincide within the measurement uncertainty in different transverse momentum ranges. A similar picture is observed for nuclear modification factors of π^0 and η mesons [28, 31]. This indicates that jet quenching in Cu + Au, Au + Au and Cu + Cu collisions at $\sqrt{s_{NN}} = 200$ GeV does not depend on the shape of the overlap region in these systems.

Conclusion

Production of K_S mesons has been measured at the PHENIX experiment in collisions of copper and gold nuclei at $\sqrt{s_{NN}} = 200$ GeV in different ranges of transverse momentum and centrality. The ratios of K_S to π^0 meson yields ($I_{KS}/I_{\pi 0}$) are independent of centrality and transverse momentum within the measurement uncertainty. The order of magnitude of the $I_{KS} / I_{\pi 0}$ ratios (0.4–0.5) coincides with similar ratios measured previously in d + Au and Cu + Cu collisions at $\sqrt{s_{NN}} = 200$ GeV in the PHENIX experiment.

Nuclear modification factors of π^0, η, and K_S mesons in (Cu + Au) collisions coincide within the measurement uncertainty in different centrality classes and transverse momentum ranges in the region $p_T > 4$–6 GeV/c, and are equal to nuclear modification factors of the jets measured in the same system in the corresponding centrality classes. This suggests that jet quenching occurs at the parton level before fragmentation in (Cu + Au) collisions.

Nuclear modification factors of K_S mesons measured in Cu + Au, Au + Au and Cu + Cu collisions at $\sqrt{s_{NN}} = 200$ GeV coincide within the measurement uncertainty in different transverse momentum ranges. This indicates that jet quenching in these systems at $\sqrt{s_{NN}} = 200$ GeV does not depend on the geometry of the overlap.

The results of this study were obtained within the framework of State Task of the Ministry of Education and Science of Russian Federation 3.1498.2017/4.6.

REFERENCES

1. **Halzen F., Martin A.D.,** Quarks and leptons: an introductory course in modern particle physics, John Wiley & sons, New York, 1984.

2. **Wang X.-N.,** Quark-gluon plasma 5, World Scientific, Beijin, 2016.

3. **Mendes M., Torrieri G.,** A quark-gluon plasma inspired model of the universe: introduction and inflation, arXiv preprint arXiv:1805.02441, 2018.

4. **Gromov N.A.,** Elementary particles in the early universe, Journal of Cosmology and Astroparticle Physics. 2016 (03) (2016) 053.

5. **Husdal L.,** On effective degrees of freedom in the early universe, Galaxies. 4 (4) (2016) 78.

6. **Arsene I., Dearden I.G., Beavis D., et al.,** Quark gluon plasma and color glass condensate at RHIC? The perspective from the BRAHMS experiment, Nuclear Physics. A. 757 (1–2) (2005) 1–27.

7. **Back B.B., Baker M.D., Ballintijn M., et**

al., The PHOBOS perspective on discoveries at RHIC, Nuclear Physics. A. 757 (1–2) (2005) 28–101.

8. **Adams J., Aggarwal M.M., Ahammed Z., et al.,** Experimental and theoretical challenges in the search for the quark gluon plasma: the STAR Collaboration's critical assessment of the evidence from RHIC collisions, Nuclear Physics. A. 757 (1–2) (2005) 102–183.

9. **Adcox K., Adler S.S., Afanasiev S., et al.,** Formation of dense partonic matter in relativistic nucleus-nucleus collisions at RHIC: experimental evaluation by the PHENIX Collaboration, Nuclear Physics. A. 757 (1–2) (2005) 184–283.

10. **Foka P., Janik M.A.,** An overview of experimental results from ultrarelativistic heavy-ion collisions at the CERN LHC: bulk properties and dynamical evolution, Reviews in Physics. 1 (November) (2016) 154–171.

11. **Miller M.L., Reygers K., Sanders S.J., et al.,** Glauber modeling in high-energy nuclear collisions, Annual Review of Nuclear and Particle Science. 57 (2007) 205–243.

12. **Adare A., Afanasiev S., Aidala C., et al.,** Inclusive cross section and double helicity asymmetry for π^0 production in $p + p$ collisions at $\sqrt{s} = 200$ GeV: implications for the polarized gluon distribution in the proton, Physical Review. D. 76 (5) (2007) 051106.

13. **Adare A., Aidala C., Ajitanand N.N., et al.,** Inclusive cross section and double-helicity asymmetry for π^0 production at midrapidity in $p + p$ collisions at $\sqrt{s} = 510$ GeV, Physical Review. D. 93 (1) (2016) 011501.

14. **Elayavalli R.K., Zapp K.C.,** Medium response in JEWEL and its impact on jet shape observables in heavy ion collisions, Journal of High Energy Physics. 2017 (7) (2017) 141.

15. **Park C., Jeon S., Gale C.,** Jet modification with medium recoil in quark-gluon plasma, Nuclear Physics. A. 982 (February) (2019) 643–646.

16. **Cao S., Luo T., Qin G.Y., et al.,** Linearized Boltzmann transport model for jet propagation in the quark-gluon plasma: heavy quark evolution, Physical Review. C. 94 (1) (2016) 014909.

17. **He Y., Luo T., Wang X.N., et al.,** Linear Boltzmann transport for jet propagation in the quark-gluon plasma: elastic processes and medium recoil, Physical Review. C. 91 (5) (2015) 054908.

18. **Chien Y.T., Vitev I.**, Towards the understanding of jet shapes and cross sections in heavy ion collisions using soft-collinear effective theory, Journal of High Energy Physics. 2016 (5) (2016) 23.

19. **Chien Y.T., Emerman A., Kang Z.B., et al.,** Jet quenching from QCD evolution, Physical Review. D. 93 (7) (2016) 074030.

20. **Cao S., Park C., Barbieri R.A., et al.,** Multistage Monte Carlo simulation of jet modification in a static medium, Physical Review. C. 96 (2) (2017) 024909.

21. **Ghiglieri J.,** Energy loss at NLO in a high-temperature Quark-Gluon Plasma, Nuclear Physics. A. 956 (December) (2016) 801–804.

22. **Djordjevic M., Zigic D., Blagojevic B., et al.,** Dynamical energy loss formalism: from describing suppression patterns to implications for future experiments, Nuclear Physics A. 982 (February) (2019) 699–702.

23. **Berdnikov A.Ya., Ivanishchev P.A., Kotov D.O., et al.,** K_s-meson suppression in central Au+Au collisions at central-of-mass energy of 200 GeV nucleon pair, St. Petersburg State Polytechnical University Journal. Physics and Mathematics. (2(122)) (2011) 111–116.

24. **Adare A., Afanasiev S., Aidala C., et al.**, Measurement of K_{S0} and K^*_0 in $p+p$, d+Au, and Cu+Cu collisions at $\sqrt{s_{NN}} = 200$ GeV, Physical Review. C. 90 (5) (2014) 054905.

25. **Adcox K., Adler S.S., Aizama M., et al.,** PHENIX detector overview, Nuclear Instruments and Methods in Physics Research. Section A: Accelerators, Spectrometers, Detectors and Associated Equipment. 499 (2–3) (2003) 469–479.

26. **Allen M., Bennett M.J., Bobrek M., et al.**, PHENIX inner detectors, Nuclear Instruments and Methods in Physics Research, Section A: Accelerators, Spectrometers, Detectors and Associated Equipment. 499 (2–3) (2003) 549–559.

27. **Aphecetche L., Awes T.C., Banning J., et al.,** PHENIX calorimeter, Nuclear Instruments and Methods in Physics Research, Section A: Accelerators, Spectrometers, Detectors and Associated Equipment. 499 (2–3) (2003) 521–536.

28. **Zharko S.** (PHENIX Collaboration), Studying parton energy loss using meson production in Large Collision Systems with PHENIX, Nuclear Physics. A. 967 (November) (2017) 552–555.

29. **Tanabashi M., Hagiwara K., Hikasa K., et al.**, Review of particle physics, Physical Review, D. 98 (3) (2018) 030001.

30. **Brun R., Hagelberg R., Hansroul M., et al.,** Geant: simulation program for particle physics experiments, User guide and reference manual, Preprint CERN, CERN-DD-78-2-REV, 1978.

31. **Aidala C., Ajitanand N.N., Akiba Y., et**

al., Production of π^0 and η mesons in Cu + Au collisions at $\sqrt{s_{NN}} = 200$ GeV, Physical Review, C. 98 (5) (2018) 054903.

32. **Adare A., Afanasiev S., Aidala C., et al.,** Measurement of neutral mesons in $p+p$ collisions at $\sqrt{s} = 200$ GeV and scaling properties of hadron production, Physical Review, D. 83 (5) (2011) 052004.

33. **Timilsina A. (**PHENIX Collaboration**),** PHENIX results on reconstructed jets in $p + p$ and Cu + Au collisions, Nuclear Physics, A. 956 (December) (2016) 637–640.

Received 22.02.2019, accepted 18.03.2019 .

THE AUTHORS

BERDNIKOV Alexander Ya.
Peter the Great St. Petersburg Polytechnic University
29 Politechnicheskaya St., St. Petersburg, 195251, Russian Federation
alexber@phmf.spbstu.ru

BERDNIKOV Yaroslav A.
Peter the Great St. Petersburg Polytechnic University
29 Politechnicheskaya St., St. Petersburg, 195251, Russian Federation
berdnikov@spbstu.ru

ZHARKO Sergei V.
Peter the Great St. Petersburg Polytechnic University
29 Politechnicheskaya St., St. Petersburg, 195251, Russian Federation
zharkosergey94@gmail.com

KOTOV Dmitry O.
Peter the Great St. Petersburg Polytechnic University
29 Politechnicheskaya St., St. Petersburg, 195251, Russian Federation
dmitriy.kotov@gmail.com

RADZEVICH Pavel V.
Peter the Great St. Petersburg Polytechnic University
29 Politechnicheskaya St., St. Petersburg, 195251, Russian Federation
radzevichp@gmail.com

СПИСОК ЛИТЕРАТУРЫ

1. Хелзен Ф., Мартин А.Д. Кварки и лепя тоны: введение в физику частиц. Пер. с англ. М.: Мир, 456 .1987 с.

2. **Wang X.-N.** (Ed.) Quark-gluon plasma 5. Beijing, China: World Scientific, 2016. 403 p.

3. **Mendes M., Torrieri G.** A quark-gluon plasma inspired model of the universe: Introduction and Inflation // arXiv preprint arXiv. 1805.02441. 2018.

4. **Gromov N.A.** Elementary particles in the early universe // Journal of Cosmology and Astroparticle Physics. 2016. Vol. 2016. No. 03. P. 053.

5. **Husdal L.** On effective degrees of freedom in the early universe // Galaxies. 2016. Vol. 4. No. 4. P. 78.

6. **Arsene I., Dearden I.G., Beavis D., et al.** Quark gluon plasma and color glass condensate at RHIC? The perspective from the BRAHMS experiment // Nuclear Physics A. 2005. Vol. 757. No. 1–2. Pp. 1–27.

7. **Back B.B., Baker M.D., Ballintijn M., et al.** The PHOBOS perspective on discoveries at RHIC // Nuclear Physics A. 2005. Vol. 757. No. 1–2. Pp. 28–101.

8. **Adams J., Aggarwal M.M., Ahammed Z., et al.** Experimental and theoretical challenges in the search for the quark gluon plasma: the STAR Collaboration's critical assessment of the evidence from RHIC collisions // Nuclear Physics A. 2005. Vol. 757. No. 1–2. Pp. 102–183.

9. **Adcox K., Adler S.S., Afanasiev S., et al.** Formation of dense partonic matter in relativistic nucleus-nucleus collisions at RHIC: experimental evaluation by the PHENIX Collabora-

tion // Nuclear Physics A. 2005. Vol. 757. No. 1–2. Pp. 184–283.

10. **Foka P., Janik M.A.** An overview of experimental results from ultrarelativistic heavy-ion collisions at the CERN LHC: bulk properties and dynamical evolution // Reviews in Physics. 2016. Vol. 1. November. Pp. 154–171.

11. **Miller M.L., Reygers, K., Sanders S. J., et al.** Glauber modeling in high-energy nuclear collisions // Annual Review of Nuclear and Particle Science. 2007. Vol. 57. Pp. 205–243.

12. **Adare A., Afanasiev S., Aidala C., et al.** Inclusive cross section and double helicity asymmetry for π^0 production in $p + p$ collisions at $\sqrt{s}$ = 200 GeV: implications for the polarized gluon distribution in the proton // Physical Review. D. 2007. Vol. 76. No. 5. P. 051106.

13. **Adare A., Aidala C., Ajitanand N.N., et al.** Inclusive cross section and double-helicity asymmetry for π^0 production at midrapidity in $p + p$ collisions at $\sqrt{s}$ = 510 GeV // Physical Review. D. 2016. Vol. 93. No. 1. P. 011501.

14. **Elayavalli R.K., Zapp K.C.** Medium response in JEWEL and its impact on jet shape observables in heavy ion collisions // Journal of High Energy Physics. 2017. Vol. 2017. No. 7. P. 141.

15. **Park C., Jeon S., Gale C.** Jet modification with medium recoil in quark-gluon plasma // Nuclear Physics. A. 2019. Vol. 982. February. Pp. 643–646.

16. **Cao S., Luo T., Qin G.Y., et al**. Linearized Boltzmann transport model for jet propagation in the quark-gluon plasma: heavy quark evolution // Physical Review. C. 2016. Vol. 94. No. 1. P. 014909.

17. **He Y., Luo T., Wang X.N., et al.** Linear Boltzmann transport for jet propagation in the quark-gluon plasma: elastic processes and medium recoil // Physical Review. C. 2015. Vol. 91. No. 5. P. 054908.

18. **Chien Y.T., Vitev I.** Towards the understanding of jet shapes and cross sections in heavy ion collisions using soft-collinear effective theory //Journal of High Energy Physics. 2016. Vol. 2016. No. 5. P. 23.

19. **Chien Y.T., Emerman A., Kang Z.B., et al.** Jet quenching from QCD evolution // Physical Review. D. 2016. Vol. 93. No. 7. P. 074030.

20. **Cao S., Park C., Barbieri R.A., et al.** Multistage Monte Carlo simulation of jet modification in a static medium // Physical Review. C. 2017. Vol. 96. No. 2. P. 024909.

21. **Ghiglieri J.** Energy loss at NLO in a high-temperature Quark-Gluon Plasma // Nuclear Physics. A. 2016. Vol. 956. December. Pp. 801–804.

22. **Djordjevic M., Zigic D., Blagojevic B., et al.** Dynamical energy loss formalism: from describing suppression patterns to implications for future experiments // Nuclear Physics. A. 2019. Vol. 982. February. Pp. 699–702.

23. Бердников А.Я., Иванищев Д.А., Котов Д.О., Рябов В.Г., Рябов Ю.Г., Самсонов В.М. Подавление выхода короткоживущих нейтральных каонов в центральных столкновениях ядер золота при энергии 200 ГэВ // Научно-технические ведомости Санкт-Петербургского государственного политехнического университета. Физико-математические науки. 122) 2 № .2011). С. 116–111.

24. **Adare A., Afanasiev S., Aidala C., et al.** Measurement of K_{S0} and K_{*0} in $p + p$, d + Au, and Cu + Cu collisions at $\sqrt{s_{NN}}$ = 200 GeV // Physical Review. C. 2014. Vol. 90. No. 5. P. 054905.

25. **Adcox K., Adler S. S., Aizama M., et al.** PHENIX detector overview // Nuclear Instruments and Methods in Physics Research. Section A: Accelerators, Spectrometers, Detectors and Associated Equipment. 2003. Vol. 499. No. 2–3. Pp. 469–479.

26. **Allen M., Bennett M. J., Bobrek M., et al.** PHENIX inner detectors // Nuclear Instruments and Methods in Physics Research. Section A: Accelerators, Spectrometers, Detectors and Associated Equipment. 2003. Vol. 499. No. 2–3. Pp. 549–559.

27. **Aphecetche L., Awes T.C., Banning J., et al.** PHENIX calorimeter // Nuclear Instruments and Methods in Physics Research. Section A: Accelerators, Spectrometers, Detectors and Associated Equipment. 2003. Vol. 499. No. 2–3. Pp. 521–536.

28. **Zharko S. (**PHENIX Collaboration**).** Studying parton energy loss using meson production in Large Collision Systems with PHENIX // Nuclear Physics. A. 2017. Vol. 967. November. Pp. 552–555.

29. **Tanabashi M., Hagiwara K., Hikasa K., et al.** Review of particle physics // Physical Review. D. 2018. Vol. 98. No. 3. P. 030001.

30. **Brun R., Hagelberg R., Hansroul M, et al.** Geant: simulation program for particle physics experiments. User guide and reference manual // Preprint CERN. CERN-DD-78-2-REV. 1978.

31. **Aidala C., Ajitanand, N.N., Akiba, Y., et al.** Production of π^0 and η mesons in Cu + Au collisions at $\sqrt{s_{NN}}$= 200 GeV // Physical Review. C. 2018. Vol. 98. No. 5. P. 054903.

32. **Adare A., Afanasiev S., Aidala C., et al.** Measurement of neutral mesons in p+p collisions at $\sqrt{s}$ = 200 GeV and scaling properties of hadron

production // Physical Review. D. 2011. Vol. 83. No. 5. P. 052004.

33. **Timilsina A. (**PHENIX Collaboration**).** PHENIX results on reconstructed jets in $p + p$ and Cu + Au collisions // Nuclear Physics. A. 2016. Vol. 956. December. Pp. 637–640.

Статья поступила в редакцию 22.02.2019, принята к публикации 18.03.2019.

СВЕДЕНИЯ ОБ АВТОРАХ

БЕРДНИКОВ Александр Ярославич – кандидат физико-математических наук, доцент кафедры экспериментальной ядерной физики Санкт-Петербургского политехнического университета Петра Великого.
195251, Российская Федерация, г. Санкт-Петербург, Политехническая ул., 29
alexber@phmf.spbstu.ru

БЕРДНИКОВ Ярослав Александрович – доктор физико-математических наук, профессор, заведующий кафедрой экспериментальной ядерной физики Санкт-Петербургского политехнического университета Петра Великого.
195251, Российская Федерация, г. Санкт-Петербург, Политехническая ул., 29
berdnikov@spbstu.ru

ЖАРКО Сергей Вячеславович – а*сс*истент кафедры экспериментальной ядерной физики Санкт-Петербургского политехнического университета Петра Великого.
195251, Российская Федерация, г. Санкт-Петербург, Политехническая ул., 29
zharkosergey94@gmail.com

КОТОВ Дмитрий Олегович – кандидат физико-математических наук, доцент кафедры экспериментальной ядерной физики Санкт-Петербургского политехнического университета Петра Великого.
195251, Российская Федерация, г. Санкт-Петербург, Политехническая ул., 29
dmitriy.kotov@gmail.com

РАДЗЕВИЧ Павел Владиславович – аспирант кафедры экспериментальной ядерной физия ки Санкт-Петербургского политехнического университета Петра Великого.
195251, Российская Федерация, г. Санкт-Петербург, Политехническая ул., 29
radzevichp@gmail.com